

## **Appendix A: Next Generation Hairpin Polyamides with (R)-3,4-**

### **Diaminobutyric Acid Turn Unit**

*The text of this chapter was taken in part from a manuscript coauthored with Christian Dose, Michelle E. Farkas, and Peter B. Dervan\* (Caltech)*

(Dose, C., Farkas, M.E., Chenoweth, D.M., and Peter B. Dervan *J. Am. Chem. Soc.*, **2008**, *130*, 6859-6866.)

**Abstract**

The characterization of a new class of pyrrole–imidazole hairpin polyamides with  $\beta$ -amino- $\gamma$ -turn units for recognition of the DNA minor groove is reported. A library of eight hairpins containing (R)- and (S)-3,4-diaminobutyric acid ( $\beta$ -amino- $\gamma$ -turn) has been synthesized, and the impact of the molecules on DNA-duplex stabilization was studied for comparison with the parent  $\gamma$ -aminobutyric acid ( $\gamma$ -turn) and standard (R)-2,4-diaminobutyric acid ( $\alpha$ -amino- $\gamma$ -turn)-linked eight-ring polyamides. For some, but not all, sequence compositions, melting temperature analyses have revealed that both enantiomeric forms of the  $\beta$ -amino- $\gamma$ -turn increase the DNA-binding affinity of polyamides relative to the (R)- $\alpha$ -amino- $\gamma$ -turn. The (R)- $\beta$ -amine residue may be an attractive alternative for constructing hairpin polyamide conjugates. Biological assays have shown that (R)- $\beta$ -amino- $\gamma$ -turn hairpins are able to inhibit androgen receptor-mediated gene expression in cell culture similar to hairpins bearing the standard (R)- $\alpha$ -amino- $\gamma$ -turn, from which we infer they are cell-permeable.

## A.1 Introduction

The ability to modulate the expression of eukaryotic gene networks by small molecules is a challenge in the field of chemical biology. Hairpin pyrrole-imidazole polyamides are a class of programmable small molecules that bind to the minor groove of DNA with affinities similar to transcription factors and have been shown to inhibit gene expression in living cells by interfering with transcription factor/DNA interfaces.<sup>1</sup> The DNA sequence specificity of polyamides arise from interactions of pairs of the aromatic amino acids *N*-methylpyrrole (Py), *N*-methylimidazole (Im), and *N*-methylhydroxypyrrole (Hp) with the edges of the Watson-Crick base pairs.<sup>2</sup> The generality of the polyamide pairing rules has been demonstrated by numerous studies<sup>3</sup> and applications of polyamide conjugates include DNA alkylations,<sup>4</sup> DNA-templated ligations,<sup>5</sup> sequence-specific DNA intercalators,<sup>6</sup> fluorescent DNA paints,<sup>7</sup> DNA nanoarchitectures,<sup>8</sup> and transcription factor mimics.<sup>9</sup> Efforts have been made to improve the DNA-binding properties of hairpin polyamides with modified turn units.<sup>10</sup> Substitution of  $\gamma$ -aminobutyric acid ( $\gamma$ -turn) by (R)-2,4-diaminobutyric acid ( $\alpha$ -amino- $\gamma$ -turn) increases the DNA-binding affinity by  $\sim 15$ -fold.<sup>10b,11</sup> In contrast, hairpins containing the opposite enantiomer, (S)- $\alpha$ -amino- $\gamma$ -turn, result in diminished binding affinities. This decrease is most likely caused by an unfavorable steric clash of the amine residue with the DNA minor groove.<sup>10b</sup> Sugiyama and co-workers have introduced polyamides containing the  $\alpha$ -hydroxy- $\gamma$ -turn.<sup>10c</sup> These hairpins provide discrimination for A•T/T•A base pairs at the turn position, although a  $\sim 70$ -fold reduced DNA-binding affinity relative to analogue (R)- $\alpha$ -amino- $\gamma$ -turn-linked polyamides has been observed.

Here we introduce a new class of hairpin polyamides which are linked by 3,4-diaminobutyric acid which results in a  $\beta$ -amine residue at the turn unit ( $\beta$ -amino- $\gamma$ -turn) (Figure A.1). DNA-binding affinities of four different eight-ring polyamide core sequences (with incrementally increasing Im/Py pairs) have been investigated and were compared to analogue hairpins bearing the parent  $\gamma$ -turn and the standard (R)- $\alpha$ -amino- $\gamma$ -turn. We show that, for certain series of hairpin polyamides, both enantiomers of the  $\beta$ -amino- $\gamma$ -turn are able to increase the relative DNA-binding affinity. However, this is sequence context dependent. Biological assays revealed that hairpin polyamides bearing the (R)- $\beta$ -amino- $\gamma$ -turn are able to inhibit specific gene expression in cell culture, which is taken as evidence for cell permeability.

## A.2 Results and Discussion

### A.2.1 Thermal stabilization of DNA duplexes by hairpin polyamides

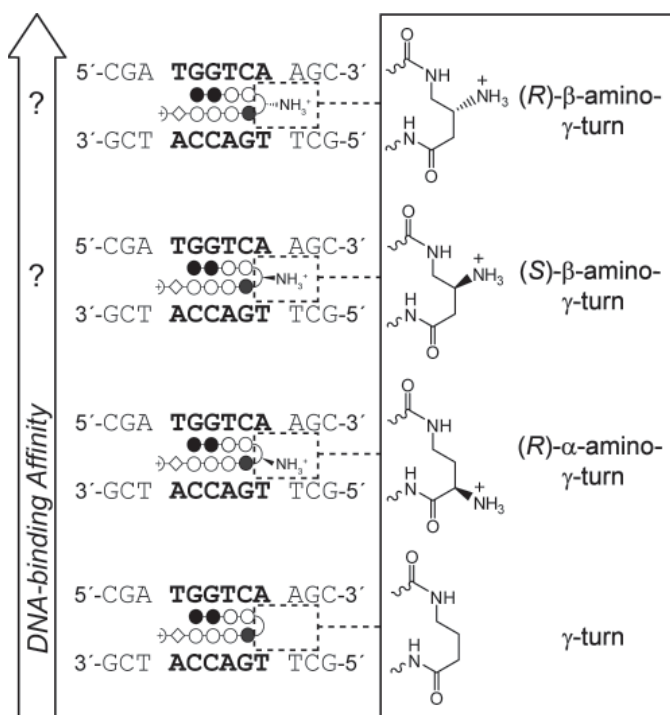


**Figure A.1** Schematic representation of hairpin polyamides with increased DNA-binding affinity caused by different  $\gamma$ -turn units. Hairpin polyamides targeted to DNA sequence 5'-TGGTCA-3' are shown as ball-and-stick models. Ball-and-stick representation legend: black and white circles represent *N*-methylimidazole and *N*-methylpyrrole units, respectively, half-circles represent  $\gamma$ -aminobutyric acid, white diamonds represent  $\beta$ -alanine units, and half-circles containing a cross represent 3-(dimethylamino)-1-propylamine (Dp) as tail.

Hairpin polyamides **1-16** were synthesized with different Im/Py and Py/Py compositions targeted to the four DNA sequences with increasing G/C content 5'-TGGTCA-3', 5'-TGGTCA-3', 5'-TGGGCA-3', and 5'-TGGGGA-3' (Figure A.2). The energetics of DNA-binding properties of polyamides are typically characterized by quantitative DNase I footprint titrations.<sup>12</sup> These measurements provide precise information regarding the affinity and specificity of DNA/polyamide complexes. Unfortunately,

quantitative footprinting experiments revealed similar equilibrium association constants ( $K_a$  values  $\sim 2 \times 10^{10} \text{ M}^{-1}$ ) for hairpins **1-8**, reaching an upper limit of the standard procedure<sup>12,13</sup> (see Section A.6 Supplemental Information). Prior results have shown that the increase in melting temperature ( $\Delta T_m$ ) of DNA

duplexes bound by hairpin polyamides correlates with DNA-binding affinity and can be utilized to detect single base pair mismatched DNA/polyamide complexes.<sup>14</sup> Accordingly, we have used melting temperature analysis for dissecting differences in DNA affinities of hairpin polyamides. Spectroscopic analyses were performed on 12mer DNA duplexes containing the appropriate match sequence in the absence and presence of polyamides in order to derive the desired  $\Delta T_m$  values (Figure A.3). Table A.1 shows that all hairpins provided an increase in melting temperature, relative to the individual DNA duplexes, confirming the formation of DNA/polyamide complexes. As expected, spectroscopic analysis with (R)- $\alpha$ -amino- $\gamma$ -turn hairpins revealed stronger stabilizations than the parent  $\gamma$ -turn analogues; for example, achiral polyamide **1** targeted to DNA sequence 5'-TGGTCA-3' resulted in a  $\Delta T_m$  value of 15.9°C, while chiral hairpin (R)- $\alpha$ -**2** led to a 3.6°C higher

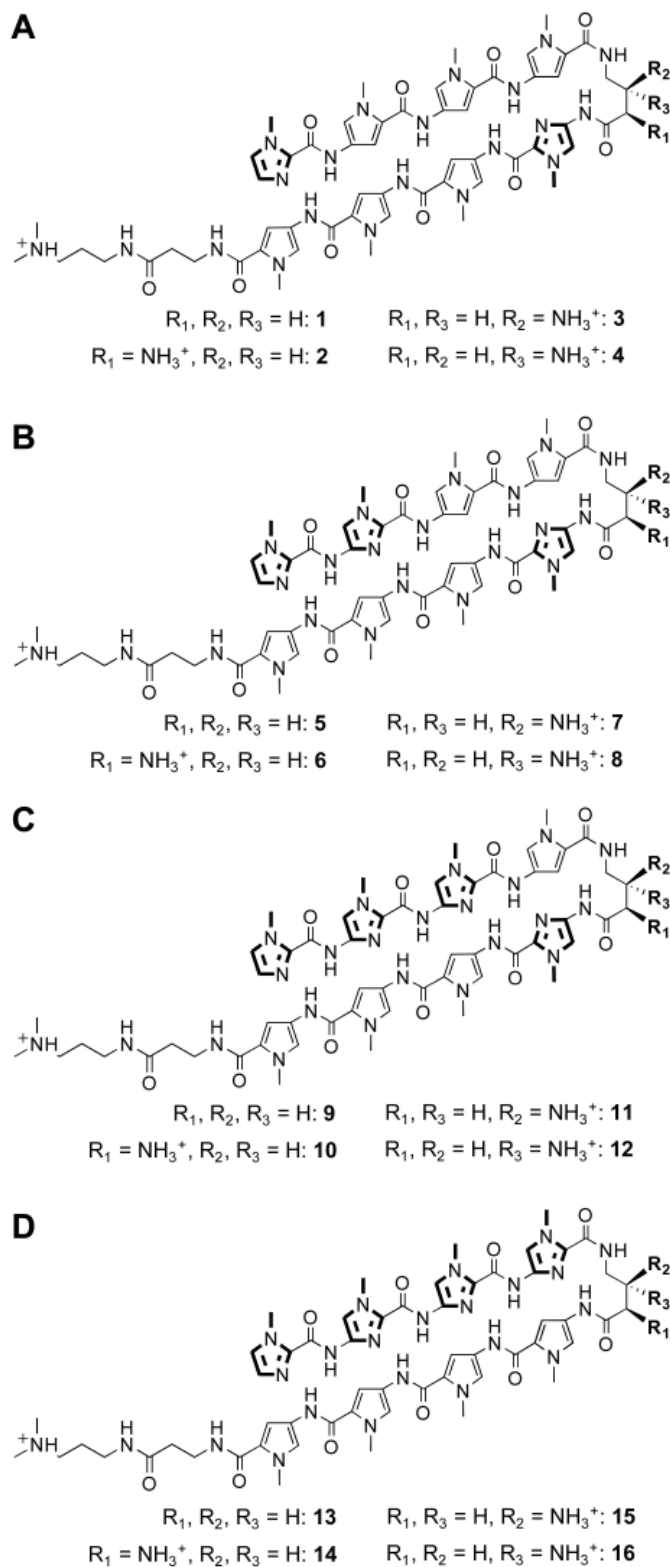


**Figure A.2** Chemical structures for hairpins **1-16** targeted to DNA sequences: (A) 5'-TGTTC A-3', (B) 5'-TGTGTC A-3', (C) 5'-TGGGCA-3', and (D) 5'-TGGGGA-3'.

melting temperature ( $\Delta T_m = 19.5^\circ\text{C}$ ). Remarkably, melting temperature analyses in the presence of  $\beta$ -amino- $\gamma$ -turn hairpins (S)- $\beta$ -**3** ( $\Delta T_m = 20.9^\circ\text{C}$ ) and (R)- $\beta$ -**4** ( $\Delta T_m = 22.2^\circ\text{C}$ ) revealed higher  $\Delta T_m$  values compared to those for the  $\alpha$ -series hairpin (R)- $\alpha$ -**2** ( $\Delta T_m = 19.5^\circ\text{C}$ ). The same trend was observed for hairpins **5-8** targeted to DNA sequence 5'-TGGTCA-3' (Table A.1, Figure A.2). First, it is noteworthy that both the (R)- and (S)- $\beta$ -amino- $\gamma$ -turn generated higher melting temperatures than the standard (R)- $\alpha$ -amino- $\gamma$ -turn. Second, the enhancement (relative to achiral hairpins) observed for the (R)- $\beta$ -series is almost twice that of the (R)- $\alpha$ -series targeted to DNA sequences 5'-TGTTC A-3' and 5'-TGGTCA-3'; for example, polyamide (R)- $\beta$ -**8** provided a  $\Delta\Delta T_m$  value of  $6.9^\circ\text{C}$ , while the  $\alpha$ -series (R)- $\alpha$ -**6** led to a  $\Delta\Delta T_m$  value of  $3.5^\circ\text{C}$  relative to achiral hairpin **5**. Interestingly, by further increasing the amounts of Im/Py pairs in the polyamides, significantly less DNA duplex stabilizations have been observed. For example, achiral polyamide **9** and chiral hairpin (R)- $\alpha$ -**10** targeted to DNA sequence 5'-TGGGCA-3' yielded  $\Delta T_m$  values of  $8.6$  and  $13.2^\circ\text{C}$ , while the  $\beta$ -series

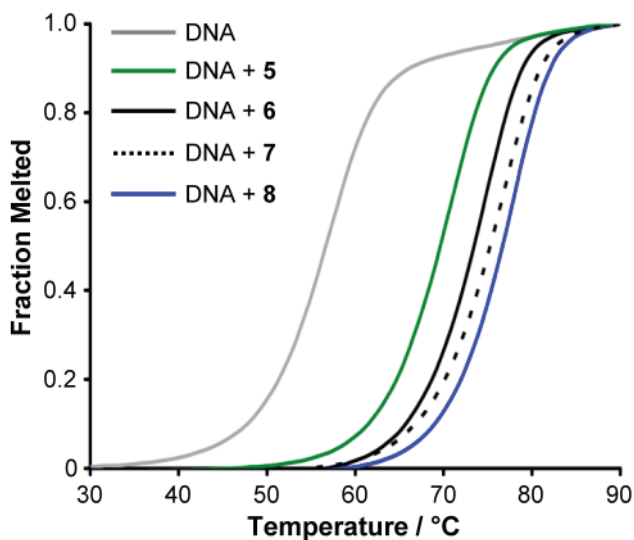


**Figure A.3** Normalized UV denaturation profiles of 12mer DNA duplex 5'-CGATGGTCAAGC-3'/5'-GCTTGACCATCG-3' in the absence and presence of hairpin polyamides **5-8**.

(S)- **$\beta$ -11** and (R)- **$\beta$ -12** led to  $\Delta T_m$  values of 13.3 and 13.6°C, respectively (Table A.1). Even lower melting temperatures were observed for hairpins **13-16** designed to bind DNA sequence 5'-TGGGGA-3'. Both  $\beta$ -amino- $\gamma$ -turns, as in (S)- **$\beta$ -15** ( $\Delta T_m = 6.7^\circ\text{C}$ ) and (R)- **$\beta$ -16** ( $\Delta T_m = 6.8^\circ\text{C}$ ), resulted in significantly lower  $\Delta T_m$  values than the  $\alpha$ -series analogue (R)- **$\alpha$ -14** ( $\Delta T_m = 9.1^\circ\text{C}$ ). These results imply that the impact of polyamide turn units on DNA-duplex stabilization is sequence context dependent.

The general increase in DNA-binding affinity for polyamides containing the (R)- $\alpha$ -substituted  $\gamma$ -turn, relative to achiral hairpins, is most likely caused by a superposition of favorable noncovalent interactions of the positively charged substituent and conformational preferences of the turn unit.<sup>10b</sup> The (R)- $\alpha$ -amino- $\gamma$ -turn can exist in two different conformations, one orienting the  $\alpha$ -ammonium in a pseudoequatorial position (Figure A.4A), which directs the substituent toward the wall of the minor groove with the potential of steric interactions. The alternate conformation places the  $\alpha$ -amine residue in a pseudoaxial position out of the minor groove, orienting the  $\beta$ -methylene to the floor of the double helix (Figure A.4B). Modeling of the (S)- $\beta$ -amino- $\gamma$ -turn conformations suggests that the  $\alpha$ -ammonium in a pseudoaxial position is directed out of the minor groove (Figure A.4C) relieving the potential steric interactions with the wall in comparison to the  $\alpha$ -series. In contrast, the (S)- $\beta$ -amine in a pseudoequatorial orientation is following the curvature of the minor groove (Figure A.4D). The possibility for favorable noncovalent interactions should exist in both conformations without the detriment of steric interactions. As shown in Figure A.4E, the pseudoequatorial  $\beta$ -amine residue of the (R)- $\beta$ -amino- $\gamma$ -turn is well accommodated in the DNA minor groove, while the pseudoaxial position should result in a steric clash of the substituent with the groove floor (Figure A.4F). Previous results have shown that polyamides constructed with several continuous Im/Py pairs are overcurved with respect to the DNA minor groove, significantly influencing the DNA binding affinity and sequence specificity.<sup>15</sup> We assume that this curvature affects the alignment of the turn units in the DNA minor groove.

**Table A.1** Melting temperatures of DNA/polyamide complexes for A•T and T•A base pairs at the turn position of hairpin polyamides.<sup>a</sup>

Polyamides	A•T		T•A	
	5'-CGA <b>TGTTCA</b> AGC-3'		5'-CGA <b>TGTTCT</b> AGC-3'	
	$T_m / ^\circ\text{C}$	$\Delta T_m / ^\circ\text{C}$	$T_m / ^\circ\text{C}$	$\Delta T_m / ^\circ\text{C}$
—	54.0 ( $\pm 0.2$ )	—	n.d.	—
 (1)	69.9 ( $\pm 0.3$ )	15.9	n.d.	—
 (2)	73.5 ( $\pm 0.2$ )	19.5	n.d.	—
 (3)	74.9 ( $\pm 0.2$ )	20.9	n.d.	—
 (4)	76.2 ( $\pm 0.2$ )	22.2	n.d.	—
—	57.2 ( $\pm 0.1$ )	—	55.8 ( $\pm 0.1$ )	—
 (5)	70.6 ( $\pm 0.2$ )	13.4	69.0 ( $\pm 0.3$ )	13.2
 (6)	74.1 ( $\pm 0.3$ )	16.9	72.9 ( $\pm 0.2$ )	17.1
 (7)	76.1 ( $\pm 0.2$ )	18.9	73.2 ( $\pm 0.1$ )	17.4
 (8)	77.5 ( $\pm 0.3$ )	20.3	74.2 ( $\pm 0.1$ )	18.4
—	60.2 ( $\pm 0.2$ )	—	59.8 ( $\pm 0.3$ )	—
 (9)	68.8 ( $\pm 0.2$ )	8.6	67.4 ( $\pm 0.3$ )	7.6
 (10)	73.4 ( $\pm 0.2$ )	13.2	72.0 ( $\pm 0.1$ )	12.2
 (11)	73.5 ( $\pm 0.1$ )	13.3	70.5 ( $\pm 0.3$ )	10.7
 (12)	73.8 ( $\pm 0.1$ )	13.6	71.3 ( $\pm 0.3$ )	11.5
—	57.5 ( $\pm 0.1$ )	—	57.9 ( $\pm 0.1$ )	—
 (13)	60.9 ( $\pm 0.1$ )	3.4	61.4 ( $\pm 0.3$ )	3.5
 (14)	66.6 ( $\pm 0.1$ )	9.1	67.0 ( $\pm 0.1$ )	9.1
 (15)	64.2 ( $\pm 0.1$ )	6.7	64.2 ( $\pm 0.1$ )	6.3
 (16)	64.3 ( $\pm 0.3$ )	6.8	64.4 ( $\pm 0.3$ )	6.5

<sup>a</sup> All values reported are derived from at least three melting temperature experiments with standard deviations indicated in parentheses (n.d. = not determined).  $\Delta T_m$  values are given as  $T_m^{(\text{DNA/polyamide})} - T_m^{(\text{DNA})}$ .

have been omitted due to the palindromic core sequence specified by the polyamides. As shown in Table A.1, most  $\gamma$ -turn and (R)- $\alpha$ -amino- $\gamma$ -turn hairpins provided similar  $\Delta T_m$  values for T•A and A•T base pairs. In contrast, significantly lower thermal stabilizations for T•A over A•T base pairs were observed for  $\beta$ -amino- $\gamma$ -turn-linked polyamides targeting DNA sequences 5'-TGGTCA-3'

This is supported by the observation that the presence of fewer continuous Im's improves the DNA affinity of  $\beta$ -amino- $\gamma$ -turns while diminishing the affinity for  $\alpha$ -amino- $\gamma$ -turns, and vice versa. However, illustrative modeling is not sufficient to explain the sequence context dependence of chiral hairpin polyamides, highlighting the pressing need for high-resolution structural studies.

#### A.2.2 Sequence specificity at the turn position

Hairpin polyamides containing the  $\gamma$ -turn have been shown to possess an equal preference for A•T/T•A over G•C/C•G base pairs at the turn position, presumably for steric reasons.<sup>16</sup> Sugiyama's  $\alpha$ -hydroxy- $\gamma$ -turns have been demonstrated to discriminate A•T versus T•A at the turn position.<sup>10c</sup> In order to study the sequence specificity for polyamides **5-16**, we performed melting temperature analyses in the presence of DNA duplexes bearing a T•A base pair at the turn position. Experiments involving hairpins **1-4**

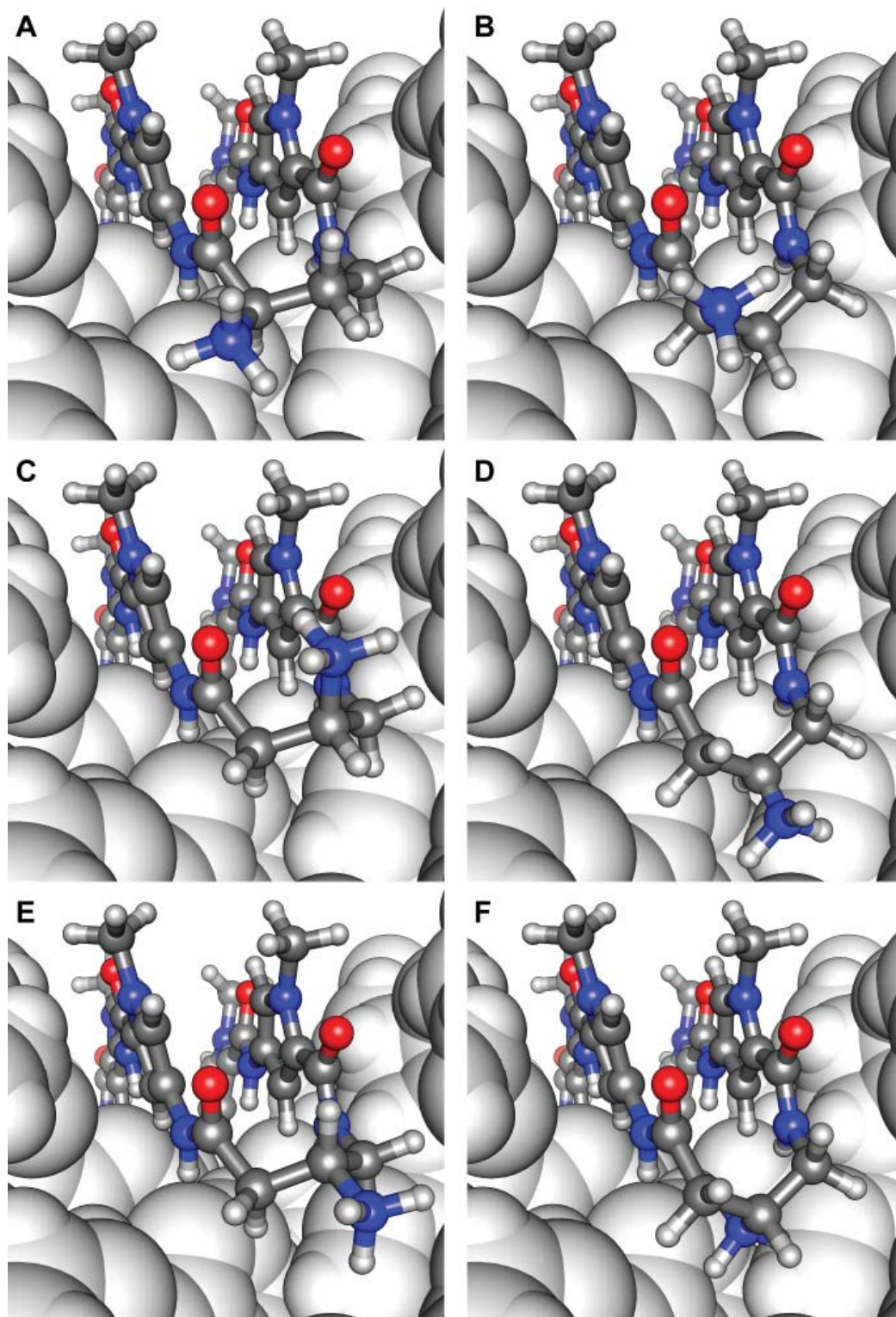
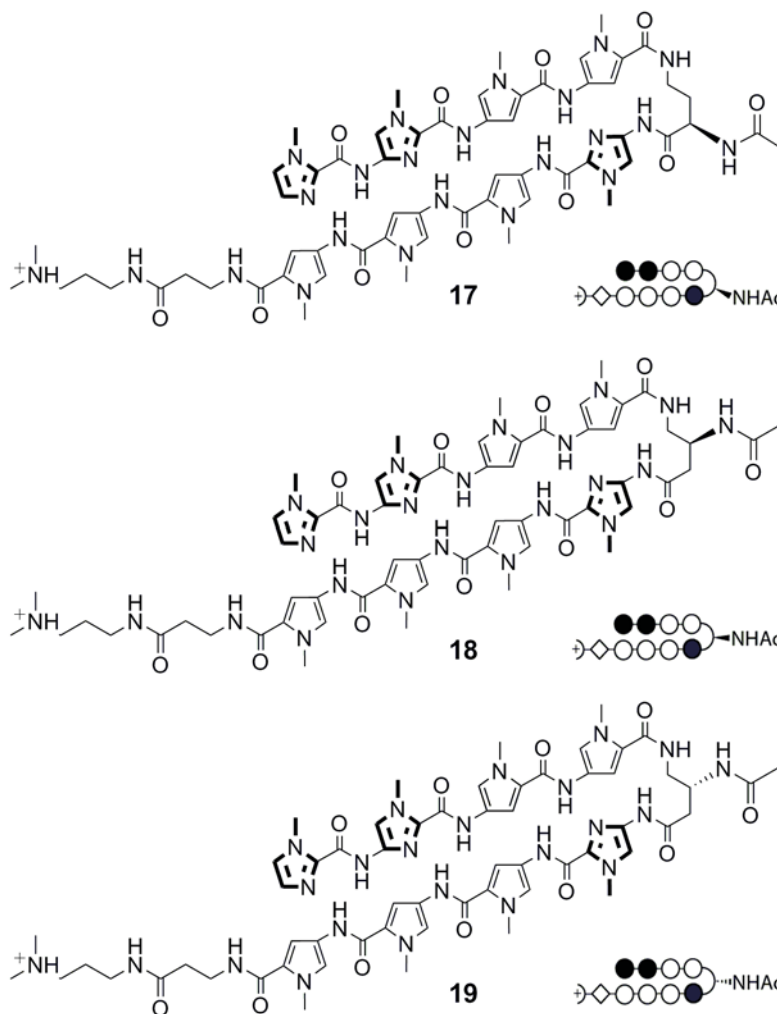


**Figure A.4** Illustrative models of different turn conformations for hairpin polyamides containing the (R)- $\alpha$ -amino- $\gamma$ -turn (A and B), (S)- $\beta$ -amino- $\gamma$ -turn (C and D), and the (R)- $\beta$ -amino- $\gamma$ -turn (E and F) bound to the minor groove of DNA (dark gray = carbons, white = hydrogen, blue = nitrogen, red = oxygen).

(5-8) and 5'-TGGGCA-3' (9-12). Even more diminished duplex stabilizations were observed in presence of C•G and G•C base pairs (see Section A.6 Supplemental Information). These observations suggest that polyamides containing  $\beta$ -amino- $\gamma$ -turns prefer A•T > T•A  $\gg$  C•G > G•C base pairs at the turn position. However, sequence specificity studies by thermal denaturation measurements require binding enthalpies ( $\Delta H_b$ ) of DNA/polyamide complexes in order to determine equilibrium association constants.<sup>14a</sup> One could also imagine using six-ring hairpin polyamides with lower DNA-binding affinities in order to discriminate sequence specificities at the turn position by quantitative DNase I footprint titration methods.

### A.2.3 Acetylated chiral hairpin polyamides

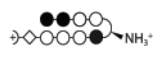
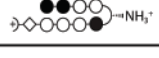
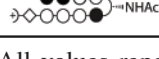
Several approaches have been reported wherein the (R)- $\alpha$ -amino- $\gamma$ -turn was utilized as a position for synthetic modifications of hairpin polyamides.<sup>4,5,17</sup> It has been shown that acetylation of the (R)- $\alpha$ -amine in six-ring hairpin polyamides results in  $\sim$ 15-fold reduced DNA-binding affinity.<sup>10b</sup> To study the tolerance of synthetic modifications for eight-ring polyamides containing the  $\beta$ -amino- $\gamma$ -turns, we examined acetylated hairpins **17-19** by melting temperature analysis (Figure A.5). Indeed, hairpin **17** containing the acetylated (R)- $\alpha$ -amino- $\gamma$ -turn yielded a markedly lower  $\Delta T_m$  value (12.8°C) than nonacetylated



**Figure A.5** Chemical structures and ball-and-stick models of acetylated hairpin polyamides **17-19** targeted to DNA sequence 5'-TGGTCA-3'.

analogue 6 ( $\Delta T_m = 16.9^\circ\text{C}$ , Table A.2). Even more pronounced was the decrease in DNA duplex stabilization for acetylated (S)- $\beta$ -amino- $\gamma$ -turn hairpin **18** leading to a  $\Delta T_m$  value of  $11.7^\circ\text{C}$ . Remarkably, the opposite enantiomer (R)- $\beta$ -**19** resulted in significantly less destabilization ( $\Delta T_m = 17.8^\circ\text{C}$ ). All hairpins lose the positive charge at the turn unit by acetylation. This implies that

**Table A.2** Melting temperatures for DNA complexes containing nonacetylated and acetylated hairpin polyamides targeted to DNA sequence 5'-TGGTCA-3'.<sup>a</sup>

DNA sequence = 5'-CGA TGGTCA AGC-3'		
Polyamides	$T_m / ^\circ\text{C}$	$\Delta T_m / ^\circ\text{C}$
—	57.2 ( $\pm 0.2$ )	—
 (6)	74.1 ( $\pm 0.3$ )	16.9
 (7)	76.1 ( $\pm 0.2$ )	18.9
 (8)	77.5 ( $\pm 0.3$ )	20.3
 (17)	70.0 ( $\pm 0.1$ )	12.8
 (18)	68.9 ( $\pm 0.2$ )	11.7
 (19)	75.0 ( $\pm 0.1$ )	17.8

<sup>a</sup> All values reported are derived from at least three melting temperature experiments with standard deviations indicated in parentheses.  $\Delta T_m$  values are given as  $T_m^{(\text{DNA/polyamide})} - T_m^{(\text{DNA})}$ .

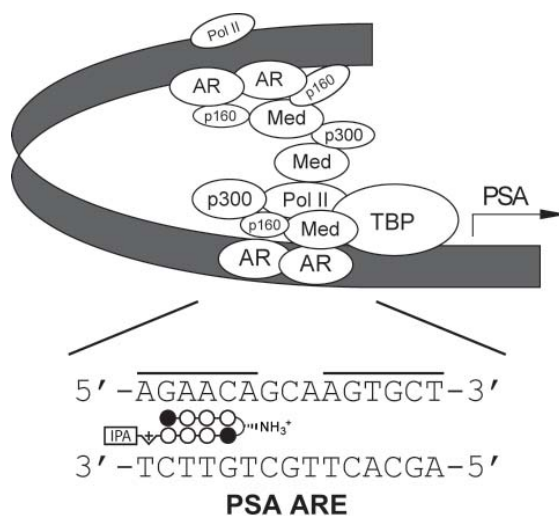


**Figure A.6** Schematic representation of the androgen receptor (AR)-mediated transcription complex with the androgen response element (ARE).

the cationic state of the amine residue is not the only contribution impacting the energetics of the DNA/polyamide complexes, as evidenced by the differences in melting temperatures between hairpins **17-19**. Increased steric demands of the acetylated substituents may also be responsible for differing binding affinities, due to the restricting DNA minor groove and alternate conformations of the  $\gamma$ -turn units (Figure A.4).

#### A.2.4 Biological assay for cell permeability

Hairpin polyamide conjugates bearing the standard (R)- $\alpha$ -amino- $\gamma$ -turn have been shown to modulate the expression of certain gene pathways in living cells by interfering with transcription factor/DNA interfaces.<sup>1</sup> Recently, a hairpin designed to bind DNA sequence 5'-AGAACA-3', found in the androgen response element (ARE), has been demonstrated to inhibit androgen receptor-mediated expression of prostate specific antigen (PSA) in LNCaP cells (Figure A.6).<sup>1b</sup> We utilized this cell culture transcription assay to investigate the cell permeability of (R)- $\beta$ -amino- $\gamma$ -turn hairpins because small structural changes within polyamides can influence nuclear uptake properties.<sup>18</sup> Hairpin polyamide **21** was examined in comparison to the previously used (R)- $\alpha$ -amino- $\gamma$ -turn hairpin

**20** (Figure A.7A). Chiral polyamides **22** and **23**, designed to target different DNA sequences, have been used as controls. Melting temperature analyses for polyamide conjugates **20-23** confirmed the results obtained for hairpins **1-4**, revealing highest DNA-duplex stabilizations for (R)- $\beta$ -amino- $\gamma$ -turn hairpins (see Section A.6 Supplemental Information). The induction of PSA mRNA by dihydrotestosterone (DHT) in LNCaP cells for matched and mismatched polyamides **20-23** was measured by quantitative real-time RT-PCR. As shown in Figure A.7B, hairpin **21** provided

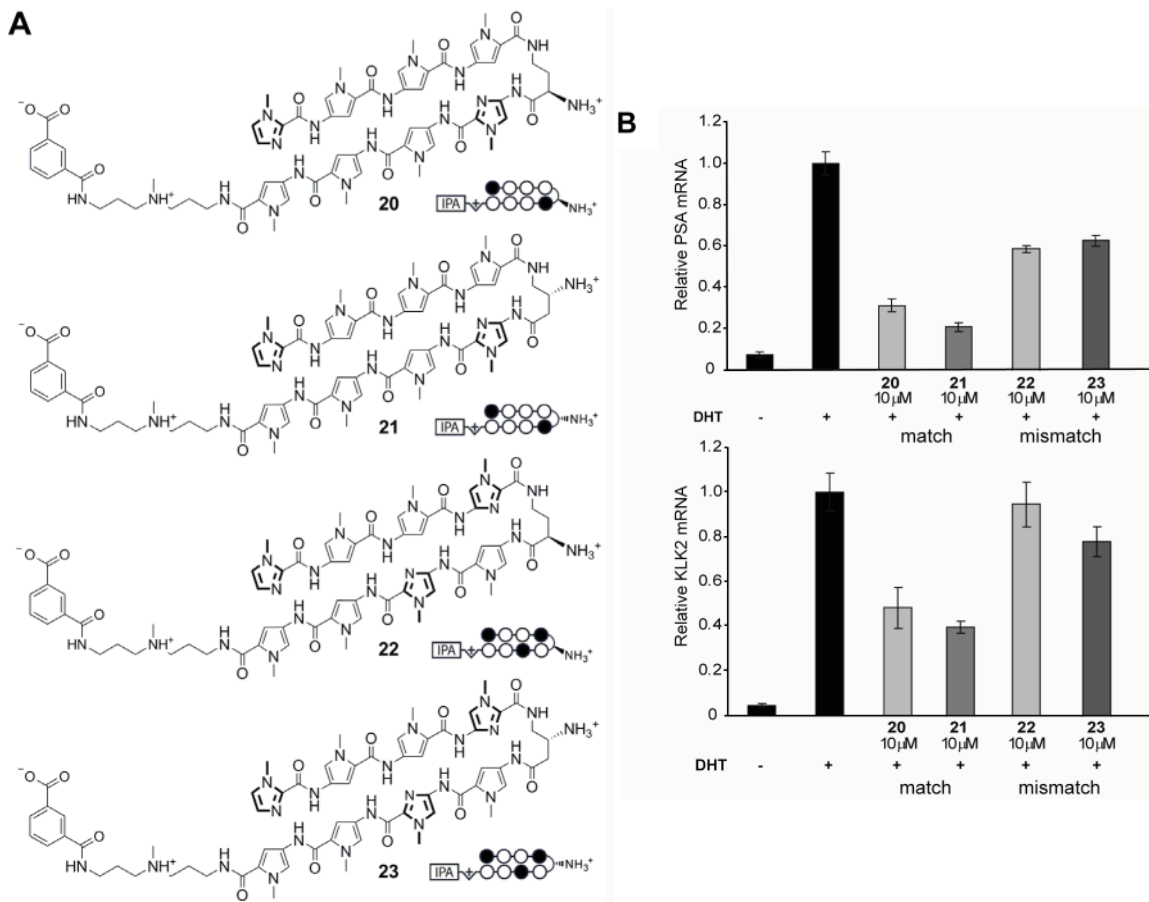


**Figure A.7** (A) Chemical structures and ball-and-stick models of matched and mismatched polyamides **20-23**, targeted to DNA sequence 5'-AGAACA-3'. (B) Inhibition of DHT-induced PSA and KLK2 expression by **20-23** measured by quantitative real-time RT-PCR

significant inhibition of AR-mediated expression of PSA mRNA, KLK2, FKBP5, and TMPRSS2 mRNA (see Section A.6 Supplemental Information) which supports cell-permeable properties for (R)- $\beta$ -amino- $\gamma$ -turn hairpins.

### A.3 Conclusion

Herein we have introduced (R)- and (S)- $\beta$ -amino- $\gamma$ -turn hairpin polyamides. Eight new polyamides targeting different DNA-binding motifs have been synthesized, and their impact on DNA duplex stabilization in relation to hairpins containing the parent  $\gamma$ -turn and the standard (R)- $\alpha$ -amino- $\gamma$ -turn was investigated. It was found that changing the turn unit from the (R)- $\alpha$ -amino- $\gamma$ -turn to either enantiomeric forms of the  $\beta$ -amino- $\gamma$ -turn increases the relative DNA-binding affinity of polyamides targeted to 5'-TGTTCA-3' and 5'-TGGTCA-3' but not to 5'-TGGGCA-3' and 5'-TGGGGA-3' sequences, rendering the impact of  $\beta$ -amino-substituted  $\gamma$ -turns sequence context dependent. Acetylation of the (S)- $\beta$ -amino- $\gamma$ -turn has been demonstrated to significantly impact the DNA-binding affinity but has minimal effect for the (R)- $\beta$ -amino- $\gamma$ -turn, which makes the (R)- $\beta$ -amino residue attractive for synthetic modifications and conjugate design. Upper limits presented by DNase I footprinting titrations of high affinity binders rendered melting temperature analysis a more practical choice for dissecting improvements by structural changes of new turn units in hairpin polyamides. Due to the strong thermal stabilizations, reported for eight-ring hairpin polyamides **1-8** targeted to 5'-TGTTCA-3' and 5'-TGGTCA-3' sequences, it is not unreasonable to estimate that the DNA-binding equilibrium association constants are markedly higher than  $K_a \sim 2 \times 10^{10} \text{ M}^{-1}$ . Biological experiments have demonstrated that (R)- $\beta$ -amino- $\gamma$ -turn hairpins possess biological activity to inhibit AR-mediated gene expression within a human cancer cell line and may have similar uptake properties as polyamides bearing the standard (R)- $\alpha$ -amino- $\gamma$ -turn. Ongoing work is focused on the use of the next generation hairpins in biological investigations as well as turn unit sequence specificity and high-resolution crystallographic studies for DNA/chiral hairpin polyamide complexes. These efforts will be reported in due course.

### A.4 Experimental

#### A.4.1 General

Chemicals and solvents were purchased from Sigma-Aldrich and were used without further purification. Boc- $\gamma$ -Abu-OH was purchased from Novabiochem. (R)-2,4-Fmoc-Dbu(Boc)-OH and Boc- $\beta$ -Ala-PAM resin were purchased from Peptides International. (R)-3,4-Cbz-Dbu(Boc)-OH and (S)-3,4-Cbz-Dbu(Boc)-OH were purchased from Senn Chemicals AG. All DNA oligomers were purchased HPLC purified from Integrated DNA Technologies. Water (18 M $\Omega$ ) was purified using a Millipore MilliQ purification system. The pH of buffers was adjusted using a Beckman 340 pH/temp meter. Analytical HPLC was performed on a Beckman Gold system equipped with a

diode array detector using a Phenomenex Gemini column (5  $\mu\text{m}$  particle size, C18 110A, 250  $\times$  4.6 mm, 5  $\mu\text{m}$ ). Preparative HPLC was performed on a Beckman Gold system equipped with a single-wavelength detector monitoring at 310 nm using a Phenomenex Gemini column (5  $\mu\text{m}$  particle size, C18 110A, 250  $\times$  21.2 mm, 5  $\mu\text{m}$ ). For both analytical and preparative HPLC, solvent A was 0.1% (v/v) aqueous trifluoroacetic acid (TFA) and solvent B was acetonitrile. Solvent gradients were adjusted as needed. Polyamide concentrations were measured in 0.1% (v/v) aqueous TFA on a Hewlett-Packard diode array spectrophotometer "Model 8452 A" and were determined by using an extinction coefficient of 69200  $\text{M}^{-1} \cdot \text{cm}^{-1}$  at  $\lambda_{\text{max}}$  near 310 nm. Matrix-assisted, LASER desorption/ionization time-of-flight mass spectrometry (MALDI-TOF MS) was performed on an Applied Biosystems Voyager DR Pro spectrometer using  $\alpha$ -cyano-4-hydroxycinnamic acid as matrix.

#### A.4.2 Synthesis of polyamides

Polyamide monomers and oligomers were synthesized as described previously.<sup>19</sup> All  $\beta$ -amino- $\gamma$ -turn hairpins were synthesized by performing the following procedure: the polyamide was cleaved from the resin with 3-(dimethylamino)-1-propylamine, purified by preparative HPLC, and characterized by MALDI-TOF MS, UV-vis spectroscopy, and analytical HPLC. A 500 nmol fraction of the Cbz-protected hairpin polyamide was dissolved in a 9:1 mixture (500  $\mu\text{L}$ ) of TFA and trifluoromethanesulfonic acid (TFMSA). After 5 min reaction time, the solution was flash-frozen by liquid  $\text{N}_2$  and overlaid with  $N,N'$ -dimethylformamide (1 mL). The thawed solution was diluted with 20% aqueous acetonitrile (8 mL), purified by preparative HPLC, and characterized by MALDI-TOF MS, UV-vis spectroscopy, and analytical HPLC. Acetylated polyamides **17-19** were synthesized by performing the following procedure: A 500 nmol fraction of the polyamide was dissolved in  $N,N'$ -dimethylformamide (900  $\mu\text{L}$ ) and a 9:1 mixture of pyridine/acetic anhydride (100  $\mu\text{L}$ ) was added. After 5 min reaction time, the solution was diluted with 10% aqueous TFA (8 mL), purified by preparative HPLC, and characterized by MALDI-TOF MS, UV-vis spectroscopy, and analytical HPLC. Polyamide conjugates **20-23** were synthesized as described previously.<sup>20</sup>

Polyamide **1**: MALDI-TOF  $[\text{M} + \text{H}]^+$  calculated for  $\text{C}_{58}\text{H}_{72}\text{N}_{21}\text{O}_{10}^+$  = 1222.6, observed = 1222.7.  
 Polyamide **2**: MALDI-TOF  $[\text{M} + \text{H}]^+$  calculated for  $\text{C}_{58}\text{H}_{73}\text{N}_{22}\text{O}_{10}^+$  = 1237.6, observed = 1237.8.  
 Polyamide **3**: MALDI-TOF  $[\text{M} + \text{H}]^+$  calculated for  $\text{C}_{58}\text{H}_{73}\text{N}_{22}\text{O}_{10}^+$  = 1237.6, observed = 1237.8.  
 Polyamide **4**: MALDI-TOF  $[\text{M} + \text{H}]^+$  calculated for  $\text{C}_{58}\text{H}_{73}\text{N}_{22}\text{O}_{10}^+$  = 1237.6, observed = 1237.8.  
 Polyamide **5**: MALDI-TOF  $[\text{M} + \text{H}]^+$  calculated for  $\text{C}_{57}\text{H}_{71}\text{N}_{22}\text{O}_{10}^+$  = 1223.6, observed = 1223.5.  
 Polyamide **6**: MALDI-TOF  $[\text{M} + \text{H}]^+$  calculated for  $\text{C}_{57}\text{H}_{72}\text{N}_{23}\text{O}_{10}^+$  = 1238.6, observed = 1238.6.

Polyamide **7**: MALDI-TOF  $[M + H]^+$  calculated for  $C_{57}H_{72}N_{23}O_{10}^+ = 1238.6$ , observed = 1238.5.  
 Polyamide **8**: MALDI-TOF  $[M + H]^+$  calculated for  $C_{57}H_{72}N_{23}O_{10}^+ = 1238.6$ , observed = 1238.5.  
 Polyamide **9**: MALDI-TOF  $[M + H]^+$  calculated for  $C_{56}H_{70}N_{23}O_{10}^+ = 1224.6$ , observed = 1224.8.  
 Polyamide **10**: MALDI-TOF  $[M + H]^+$  calculated for  $C_{56}H_{71}N_{24}O_{10}^+ = 1239.6$ , observed = 1239.6.  
 Polyamide **11**: MALDI-TOF  $[M + H]^+$  calculated for  $C_{56}H_{71}N_{24}O_{10}^+ = 1239.6$ , observed = 1239.5.  
 Polyamide **12**: MALDI-TOF  $[M + H]^+$  calculated for  $C_{56}H_{71}N_{24}O_{10}^+ = 1239.6$ , observed = 1239.6.  
 Polyamide **13**: MALDI-TOF  $[M + H]^+$  calculated for  $C_{56}H_{70}N_{23}O_{10}^+ = 1224.6$ , observed = 1224.6.  
 Polyamide **14**: MALDI-TOF  $[M + H]^+$  calculated for  $C_{56}H_{71}N_{24}O_{10}^+ = 1239.6$ , observed = 1239.7.  
 Polyamide **15**: MALDI-TOF  $[M + H]^+$  calculated for  $C_{56}H_{71}N_{24}O_{10}^+ = 1239.6$ , observed = 1239.4.  
 Polyamide **16**: MALDI-TOF  $[M + H]^+$  calculated for  $C_{56}H_{71}N_{24}O_{10}^+ = 1239.6$ , observed = 1239.5.  
 Polyamide **17**: MALDI-TOF  $[M + H]^+$  calculated for  $C_{59}H_{74}N_{23}O_{11}^+ = 1280.6$ , observed = 1280.6.  
 Polyamide **18**: MALDI-TOF  $[M + H]^+$  calculated for  $C_{59}H_{74}N_{23}O_{11}^+ = 1280.6$ , observed = 1280.7.  
 Polyamide **19**: MALDI-TOF  $[M + H]^+$  calculated for  $C_{59}H_{74}N_{23}O_{11}^+ = 1280.6$ , observed = 1280.6.  
 Polyamide **20**: MALDI-TOF  $[M + H]^+$  calculated for  $C_{65}H_{77}N_{22}O_{12}^+ = 1357.7$ , observed = 1357.6.  
 Polyamide **21**: MALDI-TOF  $[M + H]^+$  calculated for  $C_{65}H_{77}N_{22}O_{12}^+ = 1357.6$ , observed = 1357.7.  
 Polyamide **22**: MALDI-TOF  $[M + H]^+$  calculated for  $C_{64}H_{76}N_{23}O_{12}^+ = 1358.6$ , observed = 1358.6.  
 Polyamide **23**: MALDI-TOF  $[M + H]^+$  calculated for  $C_{64}H_{76}N_{23}O_{12}^+ = 1358.6$ , observed = 1358.6.

#### A.4.3 UV Absorption Spectrophotometry

Melting temperature analysis was performed on a Varian Cary 100 spectrophotometer equipped with a thermocontrolled cell holder possessing a cell path length of 1 cm. The buffer for the spectroscopic measurements was chosen to match as closely as possible the conditions of DNase I footprinting experiments. We used 10 mM sodium cacodylate since the temperature dependence of Tris-HCl makes it poorly suited for melting temperature analyses.<sup>14a</sup> A degassed aqueous solution of 10 mM sodium cacodylate, 10 mM KCl, 10 mM MgCl<sub>2</sub>, and 5 mM CaCl<sub>2</sub> at pH 7.0 was used as analysis buffer. DNA duplexes and hairpin polyamides were mixed in 1:1 stoichiometry to a final concentration of 2 μM for each experiment. Prior to analysis, samples were heated to 90 °C and cooled to a starting temperature of 25°C with a heating rate of 5°C/min for each ramp. Denaturation profiles were recorded at λ = 260 nm from 25 to 90°C with a heating rate of 0.5°C/min. The reported melting temperatures were defined as the maximum of the first derivative of the denaturation profile.

#### A.4.4 Molecular Modeling

DNA/polyamide models are based on coordinates derived from NMR structure studies using standard bond length and angles.<sup>3c</sup> The molecular graphics images are nonminimized and have been created by introducing ammonium residues to the appropriate position of the turn unit using the UCSF Chimera package from the Resource for Biocomputing, Visualization, and Informatics at the University of California, San Francisco (supported by NIH P41 RR-01081).<sup>21</sup>

#### A.4.5 Measurement of Androgen-Induced PSA mRNA

Experiments were performed as described previously.<sup>1b</sup>

### A.5 Notes and References

- (a) Olenyuk, B. Z.; Zhang, G. J.; Klco, J. M.; Nickols, N. G.; Kaelin, W. G.; Dervan, P. B. Inhibition of vascular endothelial growth factor with a sequence-specific hypoxia response element antagonist. *Proc. Natl. Acad. Sci. U. S. A.* **2004**, *101*, 16768-16773; (b) Nickols, N. G.; Dervan, P. B. Suppression of androgen receptor-mediated gene expression by a sequence-specific DNA-binding polyamide. *Proc. Natl. Acad. Sci. U. S. A.* **2007**, *104*, 10418-10423; (c) Nickols, N. G.; Jacobs, C. S.; Farkas, M. E.; Dervan, P. B. Modulating hypoxia-inducible transcription by disrupting the HIF-1-DNA interface. *ACS Chemical Biology* **2007**, *2*, 561-571.
- (a) Dervan, P. B. Molecular recognition of DNA by small molecules. *Bioorg. Med. Chem.* **2001**, *9*, 2215-2235; (b) Dervan, P. B.; Edelson, B. S. Recognition of the DNA minor groove by pyrrole-imidazole polyamides. *Curr. Opin. Struct. Biol.* **2003**, *13*, 284-299.
- (a) Kielkopf, C. L.; White, S.; Szewczyk, J. W.; Turner, J. M.; Baird, E. E.; Dervan, P. B.; Rees, D. C. A structural basis for recognition of A•T and T•A base pairs in the minor groove of B-DNA. *Science* **1998**, *282*, 111-115; (b) Kielkopf, C. L.; Baird, E. E.; Dervan, P. D.; Rees, D. C. Structural basis for G•C recognition in the DNA minor groove. *Nat. Struct. Biol.* **1998**, *5*, 104-109; (c) Zhang, Q.; Dwyer, T. J.; Tsui, V.; Case, D. A.; Cho, J. H.; Dervan, P. B.; Wemmer, D. E. NMR structure of a cyclic polyamide-DNA complex. *J. Am. Chem. Soc.* **2004**, *126*, 7958-7966; (d) Puckett J. W.; Muzikar K. A.; Tietjen J.; Warren C. L.; Ansari A. Z.; Dervan P. B. Quantitative Microarray Profiling of DNA-Binding Molecules. *J. Am. Chem. Soc.* **2007**, *129*, 12310-12319.
- (a) Wurtz, N. R.; Dervan, P. B. Sequence specific alkylation of DNA by hairpin pyrrole-imidazole polyamide conjugates. *Chemistry & Biology* **2000**, *7*, 153-161; (b) Sasaki, S.; Bando, T.; Minoshima, M.; Shimizu, T.; Shinohara, K.; Takaoka, T.; Sugiyama, H. Sequence-specific alkylation of double-strand human telomere repeat sequence by pyrrole-imidazole polyamides with indole linkers. *J. Am. Chem. Soc.* **2006**, *128*, 12162-12168; (c) Tsai, S. M.; Farkas, M. E.; Chou, C. J.; Gottesfeld, J. M.; Dervan, P. B. Unanticipated differences between alpha- and gamma-diaminobutyric acid-linked hairpin polyamide-alkylator conjugates. *Nucleic Acids Res.* **2007**, *35*, 307-316; (d) Minoshima, M.; Bando, T.; Sasaki, S.; Shinohara, K.; Shimizu, T.; Fujimoto, J.; Sugiyama, H. DNA alkylation by pyrrole-imidazole seco-CBI conjugates with an indole linker: sequence-specific DNA alkylation with 10-base-pair recognition through heterodimer formation. *J. Am. Chem. Soc.* **2007**, *129*, 5384-5390.
- Poulin-Kerstien, A. T.; Dervan, P. B. A two-hit mechanism for pre-mitotic arrest of cancer cell proliferation by a polyamide-alkylator conjugate. *J. Am. Chem. Soc.* **2003**, *125*, 15811-15821.

6. (a) Fechter, E. J.; Dervan, P. B. Allosteric inhibition of protein--DNA complexes by polyamide-intercalator conjugates. *J. Am. Chem. Soc.* **2003**, *125*, 8476-8485; (b) Fechter, E. J.; Olenyuk, B.; Dervan, P. B. Design of a sequence-specific DNA bisintercalator. *Angew. Chem. Int. Ed.* **2004**, *43*, 3591-3594; (c) Fechter E. J.; Olenyuk B.; Dervan P. B. Sequence-specific fluorescence detection of DNA by polyamide-thiazole orange conjugates. *J. Am. Chem. Soc.* **2005**, *127*, 16685-16691.
7. (a) Rucker V. C.; Foister S.; Melander C.; Dervan P. B. Sequence specific fluorescence detection of double strand DNA. *J. Am. Chem. Soc.* **2003**, *125*, 1195-1202; (b) Chenoweth, D. M.; Viger, A.; Dervan, P. B. Fluorescent sequence-specific dsDNA binding oligomers. *J. Am. Chem. Soc.* **2007**, *129*, 2216-2217.
8. (a) Cohen, J. D.; Sadowski, J. P.; Dervan, P. B. Addressing single molecules on DNA nanostructures. *Angew. Chem. Int. Ed.* **2007**, *46*, 7956-7959; (b) Schmidt, T. L.; Nandi, C. K.; Rasched, G.; Parui, P. P.; Brutschy, B.; Famulok, M.; Heckel, A. Polyamide struts for DNA architectures. *Angew. Chem. Int. Ed.* **2007**, *46*, 4382-4384; (c) Cohen J. D.; Sadowski J. P.; Dervan P. B. Programming multiple protein patterns on a single DNA nanostructure. *J. Am. Chem. Soc.* **2008**, *130*, 402-403.
9. (a) Arndt, H. D.; Hauschild, K. E.; Sullivan, D. P.; Lake, K.; Dervan, P. B.; Ansari, A. Z. Toward artificial developmental regulators. *J. Am. Chem. Soc.* **2003**, *125*, 13322-13323; (b) Kwon, Y.; Arndt, H. D.; Qian, M.; Choi, Y.; Kawazoe, Y.; Dervan, P. B.; Uesugi, M. Small molecule transcription factor mimic. *J. Am. Chem. Soc.* **2004**, *126*, 15940-15941; (c) Hauschild, K. E.; Metzler, R. E.; Arndt, H. D.; Moretti, R.; Raffaele, M.; Dervan, P. B.; Ansari, A. Z. Temperature-sensitive protein-DNA dimerizers. *Proc. Natl. Acad. Sci. U. S. A.* **2005**, *102*, 5008-5013; (d) Stafford, R. L.; Arndt, H. D.; Brezinski, M. L.; Ansari, A. Z.; Dervan, P. B. Minimization of a protein-DNA dimerizer. *J. Am. Chem. Soc.* **2007**, *129*, 2660-2668; (e) Stafford, R. L.; Dervan, P. B. The reach of linear protein-DNA dimerizers. *J. Am. Chem. Soc.* **2007**, *129*, 14026-14033; (f) Xiao, X.; Yu, P.; Lim, H. S.; Sikder, D.; Kodadek, T. A cell-permeable synthetic transcription factor mimic. *Angew. Chem. Int. Ed.* **2007**, *46*, 2865-2868.
10. (a) Mrksich, M.; Parks, M. E.; Dervan, P. B. Hairpin peptide motif. A new class of oligopeptides for sequence-specific recognition in the minor groove of double-helical DNA. *J. Am. Chem. Soc.* **1994**, *116*, 7983-7988; (b) Herman, D. M.; Baird, E. E.; Dervan, P. B. Stereochemical control of the DNA binding affinity, sequence specificity, and orientation preference of chiral hairpin polyamides in the minor groove. *J. Am. Chem. Soc.* **1998**, *120*, 1382-1391; (c) Zhang, W.; Minoshima, M.; Sugiyama, H. Base pair recognition of the stereochemically alpha-substituted gamma-turn of pyrrole/imidazole hairpin polyamides. *J. Am. Chem. Soc.* **2006**, *128*, 14905-14912; (d) Farkas, M. E.; Tsai, S. M.; Dervan, P. B. Alpha-diaminobutyric acid-linked hairpin polyamides. *Bioorg. Med. Chem.* **2007**, *15*, 6927-6936.
11. Hsu, C. F.; Phillips, J. W.; Trauger, J. W.; Farkas, M. E.; Belitsky, J. M.; Heckel, A.; Olenyuk, B. Z.; Puckett, J. W.; Wang, C. C. C.; Dervan, P. B. Completion of a programmable DNA-binding small molecule library. *Tetrahedron* **2007**, 6146-6151.
12. Trauger, J. W.; Dervan, P. B. Footprinting methods for analysis of pyrrole-imidazole polyamide/DNA complexes. *Methods Enzymol.* **2001**, *340*, 450-466.
13. For quantitative footprinting experiments, the DNA concentrations of equilibrium mixtures should be at least 10-fold less than the total association constant of the DNA/ligand complex in order to ensure the approximation  $[\text{ligand}]_{\text{free}} = [\text{ligand}]_{\text{total}}$  for numerical analysis. However, the concentration of the labeled DNA fragment specified by the standard DNA/polyamide footprinting protocol is  $\sim 5$  pM.<sup>12</sup> Consequently, DNA-association constants become compressed and hence unreliable for comparison studies at  $K_a$  values  $\geq 2 \times 10^{10} \text{ M}^{-1}$ . (a) Brenowitz, M.; Senear, D. F.;

- Shea, M. A.; Ackers, G. K. Quantitative DNase footprint titration: a method for studying protein-DNA interactions. *Methods Enzymol.* **1986**, *130*, 132-181; (b) Senear, D. F.; Dalma-Weiszhausz, D. D.; Brenowitz, M. Effects of anomalous migration and DNA to protein ratios on resolution of equilibrium constants from gel mobility-shift assays. *Electrophoresis* **1993**, *14*, 704-712.
14. (a) Pilch, D. S.; Poklar, N.; Gelfand, C. A.; Law, S. M.; Breslauer, K. J.; Baird, E. E.; Dervan, P. B. Binding of a hairpin polyamide in the minor groove of DNA: Sequence-specific enthalpic discrimination. *Proc. Natl. Acad. Sci. U. S. A.* **1996**, *93*, 8306-8311; (b) Pilch, D. S.; Poklar, N.; Baird, E. E.; Dervan, P. B.; Breslauer, K. J. The thermodynamics of polyamide-DNA recognition: hairpin polyamide binding in the minor groove of duplex DNA. *Biochemistry* **1999**, *38*, 2143-2151.
15. (a) Turner, J. M.; Swalley, S. E.; Baird, E. E.; Dervan, P. B. Aliphatic/aromatic amino acid pairings for polyamide recognition in the minor groove of DNA. *J. Am. Chem. Soc.* **1998**, *120*, 6219-6226; (b) Floreancig, P. E.; Swalley, S. E.; Trauger, J. W.; Dervan, P. B. Recognition of the minor groove of DNA by hairpin polyamides containing  $\alpha$ -substituted- $\beta$ -amino acids. *J. Am. Chem. Soc.* **2000**, *122*, 6342-6350.
16. Swalley, S. E.; Baird, E. E.; Dervan, P. B. Effects of gamma-turn and beta-tail amino acids on sequence-specific recognition of DNA by hairpin polyamides. *J. Am. Chem. Soc.* **1999**, *121*, 1113-1120.
17. (a) Weyermann, P.; Dervan, P. B. Recognition of ten base pairs of DNA by head-to-head hairpin dimers. *J. Am. Chem. Soc.* **2002**, *124*, 6872-6878; (b) Herman, D. M.; Baird, E. E.; Dervan, P. B. Tandem hairpin motif for recognition in the minor groove of DNA by pyrrole-imidazole polyamides. *Chem. Eur. J.* **1999**, *5*, 975-983; (c) Wang, C. C. C.; Dervan, P. B. Sequence-specific trapping of topoisomerase I by DNA binding polyamide-camptothecin conjugates. *J. Am. Chem. Soc.* **2001**, *123*, 8657-8661; (d) Edayathumangalam, R. S.; Weyermann, P.; Gottesfeld, J. M.; Dervan, P. B.; Luger, K. Molecular recognition of the nucleosomal "supergroove". *Proc. Natl. Acad. Sci. U. S. A.* **2004**, *101*, 6864-6869.
18. (a) Best, T. P.; Edelson, B. S.; Nickols, N. G.; Dervan, P. B. Nuclear localization of pyrrole-imidazole polyamide-fluorescein conjugates in cell culture. *Proc. Natl. Acad. Sci. U. S. A.* **2003**, *100*, 12063-12068; (b) Edelson, B. S.; Best, T. P.; Olenyuk, B.; Nickols, N. G.; Doss, R. M.; Foister, S.; Heckel, A.; Dervan, P. B. Influence of structural variation on nuclear localization of DNA-binding polyamide-fluorophore conjugates. *Nucleic Acids Res.* **2004**, *32*, 2802-2818.
19. Baird, E. E.; Dervan, P. B. Solid phase synthesis of polyamides containing imidazole and pyrrole amino acids. *J. Am. Chem. Soc.* **1996**, *118*, 6141-6146.
20. Nickols, N. G.; Jacobs, C. S.; Farkas, M. E.; Dervan, P. B. Improved nuclear localization of DNA-binding polyamides. *Nucleic Acids Res.* **2007**, *35*, 363-370.
21. Pettersen, E. F.; Goddard, T. D.; Huang, C. C.; Couch, G. S.; Greenblatt, D. M.; Meng, E. C.; Ferrin, T. E. UCSF Chimera – A visualization system for exploratory research and analysis. *J. Comput. Chem.* **2004**, *25*, 1605-1612.

## A.6 Supplemental Information

Construction of Plasmids pCDMF-1 and pCDMF-2: Oligonucleotides were purchased from Integrated DNA Technologies. The plasmids pCDMF-1 and pCDMF-2 were constructed by annealing the oligonucleotides: 5'-AGCTGCGGCTCGAGACGGCTAACCCATCGAGACGGCTAGCCCATCG-AGACGGCTATCCCATCGAGACGGCTACCCCATCGAGAGGATC-3' and 5-GATCGATCCTCT-CGATGGGGTAGCCGTCTCGATGGGATAGCCGTCTCGATGGGGCTAGCCGTCTCGATGGGGTTA-GCCGTCTCGAGCCGC-3'; 5'-AGCTGCGAGACGGCTCGAGACGGCTTGAACATCGAGACGG-CTCGAGACGGCTTGACCATCGAGACGGCTCGAGACGGCTC-3' and 5-GATCGAGCCGTCTCG-AGCCGTCTCGATGGTCAAGCCGTCTCGAGCCGTCTCGATGTTCAAGCCGTCTCGAGCCGTCTCGC-3', respectively, followed by ligation into the BamHI/HindIII restriction fragment of pUC19 using T4 DNA ligase. The plasmid was then transformed into Escherichia coli JM109 competent cells. Ampicillin-resistant white colonies were selected from 25 mL Luria–Bertani (LB) agar plates containing 50 mg/mL ampicillin treated with XGAL and isopropyl-β-D-thiogalactopyranoside (IPTG) solutions and grown overnight at 37°C. Cells were harvested the following day and purification of the plasmid was performed with a Wizard Plus Midiprep DNA purification kit (Promega). DNA sequencing of the plasmid insert was performed by the sequence analysis facility at the California Institute of Technology.

DNase I Footprinting Titrations: Polyamide equilibrations and DNase I footprint titrations were conducted on the 5' end-labeled PCR product of pCDMF-1 and pCDMF-2 according to standard protocols.<sup>12</sup> DNA was incubated with polyamides or water (control) for 12 h at room temperature prior to reaction with DNase I.

**Table A.3** Melting temperatures of DNA/polyamide complexes for all four base pair variations at the turn position of hairpin polyamides.<sup>a</sup>

Polyamides	A•T		T•A		C•G		G•C	
	5'-CGA TGGTCA AGC-3'		5'-CGA TGGTCT AGC-3'		5'-CGA TGGTCC AGC-3'		5'-CGA TGGTCG AGC-3'	
	$T_m / ^\circ\text{C}$	$\Delta T_m / ^\circ\text{C}$	$T_m / ^\circ\text{C}$	$\Delta T_m / ^\circ\text{C}$	$T_m / ^\circ\text{C}$	$\Delta T_m / ^\circ\text{C}$	$T_m / ^\circ\text{C}$	$\Delta T_m / ^\circ\text{C}$
—	57.2 (±0.1)	—	55.8 (±0.1)	—	59.7 (±0.3)	—	60.4 (±0.2)	—
(5)	70.6 (±0.2)	13.4	69.0 (±0.3)	13.2	65.9 (±0.3)	6.2	64.3 (±0.1)	3.9
(6)	74.1 (±0.3)	16.9	72.9 (±0.2)	17.1	67.3 (±0.2)	7.6	64.7 (±0.2)	4.3
(7)	76.1 (±0.2)	18.9	73.2 (±0.1)	17.4	69.7 (±0.3)	10.0	66.1 (±0.2)	5.7
(8)	77.5 (±0.3)	20.3	74.2 (±0.1)	18.4	70.1 (±0.1)	10.4	66.8 (±0.2)	6.4

<sup>a</sup> All values reported are derived from at least three melting temperature experiments with standard deviations indicated in parentheses (n.d. = not determined).  $\Delta T_m$  values are given as  $T_m^{(\text{DNA/polyamide})} - T_m^{(\text{DNA})}$ .

**Table A.4** Equilibrium association constants for hairpin polyamides determined by quantitative DNase I footprint titrations.<sup>a</sup>

Polyamides	A•T		T•A	
	5'-CGA <b>TGTTCA</b> AGC-3'		5'-CGA <b>TGTTCT</b> AGC-3'	
	$K_a / M^{-1}$		$K_a / M^{-1}$	
 (1)	3.0 ( $\pm 0.8$ ) $\times 10^{10}$ <sup>[b]</sup>		n. d.	
 (2)	2.6 ( $\pm 0.6$ ) $\times 10^{10}$		n. d.	
 (3)	2.1 ( $\pm 0.1$ ) $\times 10^{10}$		n. d.	
 (4)	2.7 ( $\pm 0.3$ ) $\times 10^{10}$		n. d.	
		5'-CGA <b>TGGTCA</b> AGC-3'	5'-CGA <b>TGGTCT</b> AGC-3'	
 (5)	1.3 ( $\pm 0.7$ ) $\times 10^{10}$ <sup>[b]</sup>		n. d.	
 (6)	3.1 ( $\pm 0.5$ ) $\times 10^{10}$		n. d.	
 (7)	2.4 ( $\pm 0.3$ ) $\times 10^{10}$		n. d.	
 (8)	2.3 ( $\pm 0.3$ ) $\times 10^{10}$		n. d.	
		5'-CGA <b>TGGGCA</b> AGC-3'	5'-CGA <b>TGGGCT</b> AGC-3'	
 (9)	n. d.		n. d.	
 (10)	n. d.		1.5 ( $\pm 0.2$ ) $\times 10^{10}$	
 (11)	n. d.		3.0 ( $\pm 0.4$ ) $\times 10^9$	
 (12)	n. d.		5.9 ( $\pm 0.9$ ) $\times 10^9$	
		5'-CGA <b>TGGGGA</b> AGC-3'	5'-CGA <b>TGGGGT</b> AGC-3'	
 (13)	2.8 ( $\pm 0.2$ ) $\times 10^7$ <sup>[b]</sup>		n. d.	
 (14)	n. d.		6.6 ( $\pm 1.8$ ) $\times 10^9$	
 (15)	n. d.		9.4 ( $\pm 3.0$ ) $\times 10^7$	
 (16)	n. d.		2.1 ( $\pm 0.6$ ) $\times 10^8$	

<sup>a</sup> Equilibrium association constants reported are mean values from at least three quantitative DNase I footprint titration experiments. Standard deviations are shown in parentheses. <sup>b</sup> Equilibrium association constants have been reported previously<sup>11</sup> (n. d. = not determined).

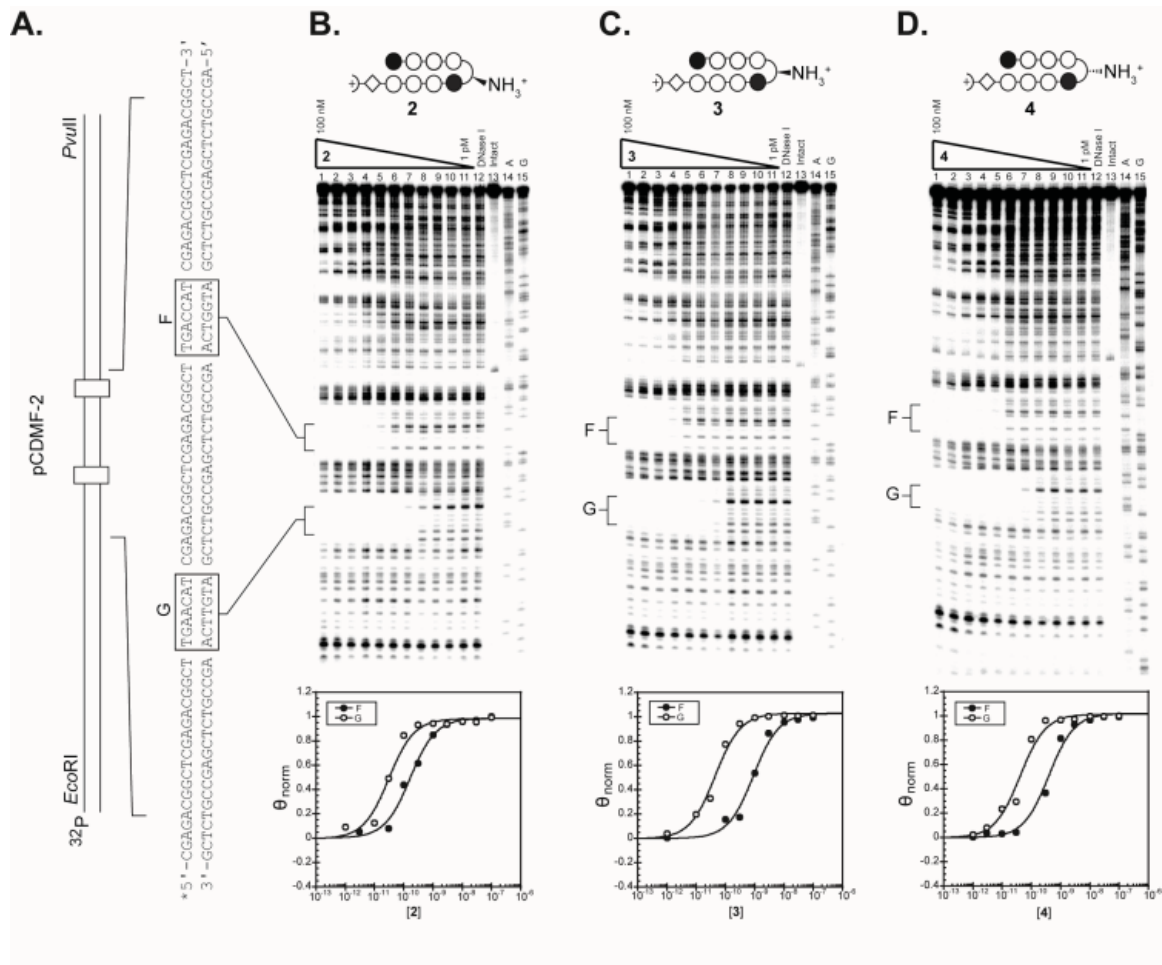


**Figure A.8** Quantitative DNase I footprint titration experiments for polyamides **2**, **3**, and **4** on the 285 base pair, 5' end-labeled PCR product of plasmid pCDMF-2: lanes 1-11, 100 nM, 30 nM, 3 nM, 1 nM, 300 pM, 100 pM, 30 pM, 10 pM, 3 pM, and 1 pM polyamide, respectively; lane 12, DNase I standard; lane 13, intact DNA; lane 14, A reaction; lane 15, G reaction.

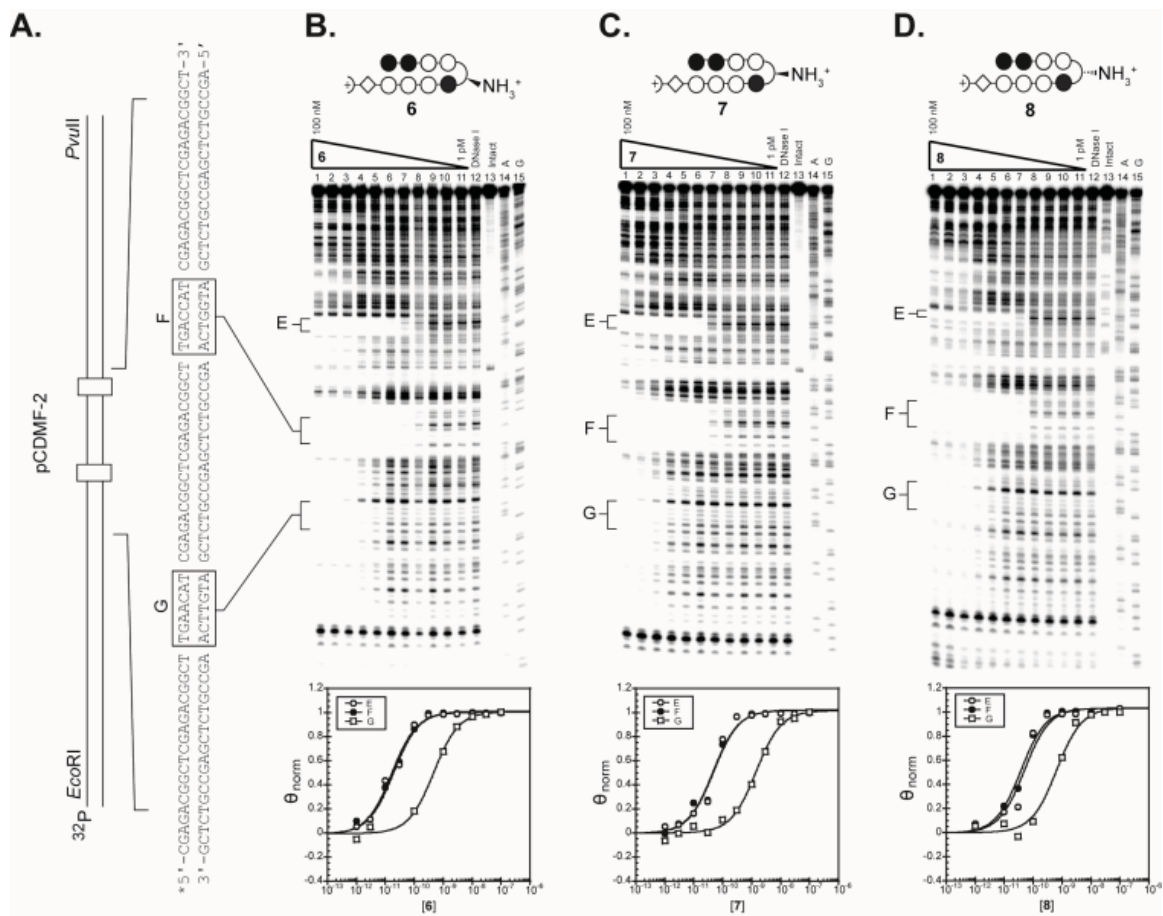


**Figure A.9** Quantitative DNase I footprint titration experiments for polyamides **6**, **7**, and **8** on the 285 base pair, 5' end-labeled PCR product of plasmid pCDMF-2: lanes 1-11, 100 nM, 30 nM, 3 nM, 1 nM, 300 pM, 100 pM, 30 pM, 10 pM, 3 pM, and 1 pM polyamide, respectively; lane 12, DNase I standard; lane 13, intact DNA; lane 14, A reaction; lane 15, G reaction.



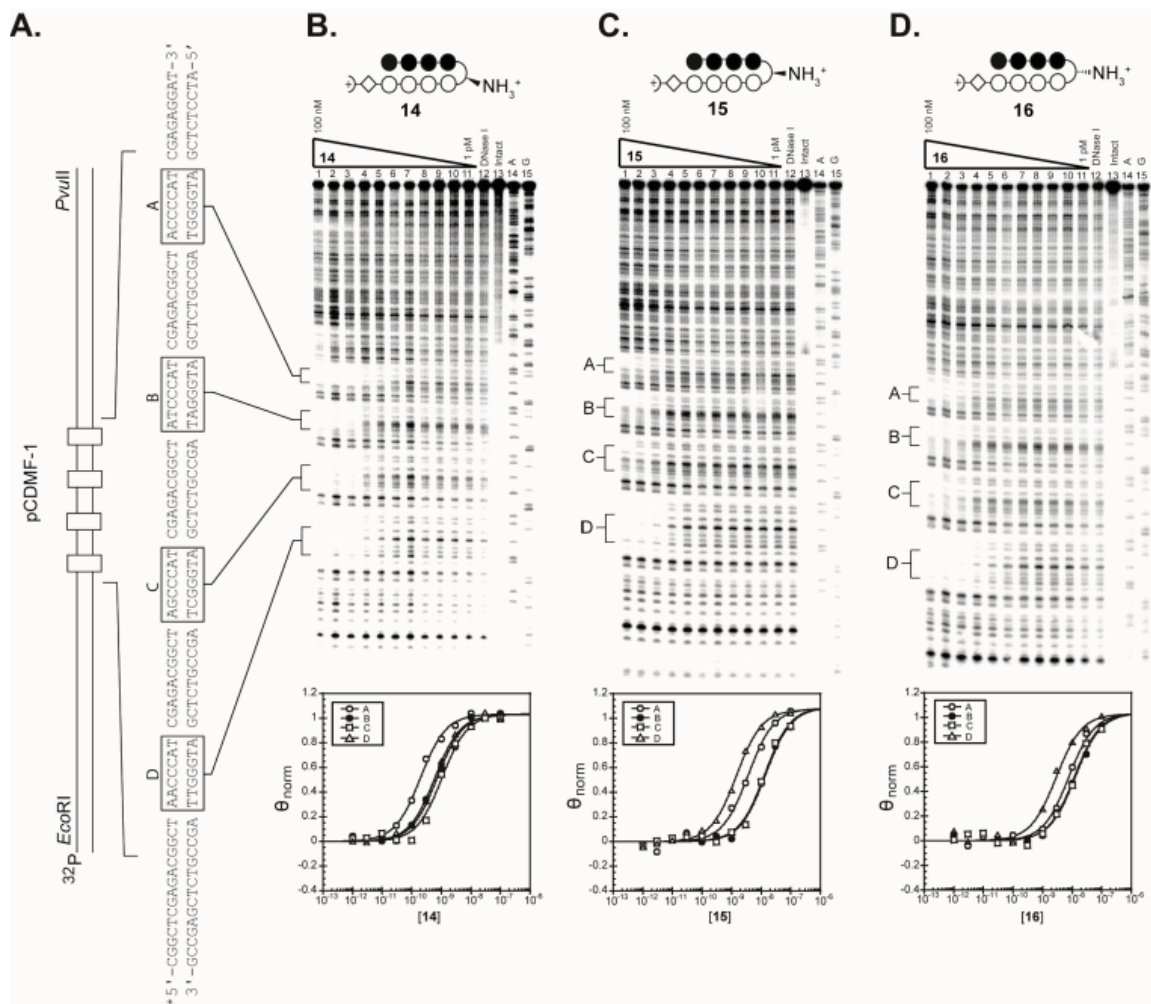


**Figure A.11** Quantitative DNase I footprint titration experiments for polyamides **14**, **15**, and **16** on the 293 base pair, 5' end-labeled PCR product of plasmid pCDMF-1: lanes 1-11, 100 nM, 30 nM, 3 nM, 1 nM, 300 pM, 100 pM, 30 pM, 10 pM, 3 pM, and 1 pM polyamide, respectively; lane 12, DNase I standard; lane 13, intact DNA; lane 14, A reaction; lane 15, G reaction.

**Table A.5** Melting temperatures of polyamides targeted to DNA-sequence 5'-AGAACA-3' in complex with DNA.<sup>a</sup>

DNA sequence = 5'-TTGC <b>AGAACA</b> GCAA-3'		
Polyamides	$T_m / ^\circ\text{C}$	$\Delta T_m / ^\circ\text{C}$
—	60.1 ( $\pm 0.2$ )	—
 <b>(20)</b>	74.4 ( $\pm 0.2$ )	14.3
 <b>(21)</b>	76.3 ( $\pm 0.2$ )	16.2
 <b>(22)</b>	64.6 ( $\pm 0.1$ )	4.5
 <b>(23)</b>	66.9 ( $\pm 0.1$ )	6.8

<sup>a</sup> All values reported are derived from at least three melting temperature experiments with standard deviations indicated in parentheses.  $\Delta T_m$  values are given as  $T_m^{(\text{DNA/polyamide})} - T_m^{(\text{DNA})}$ .

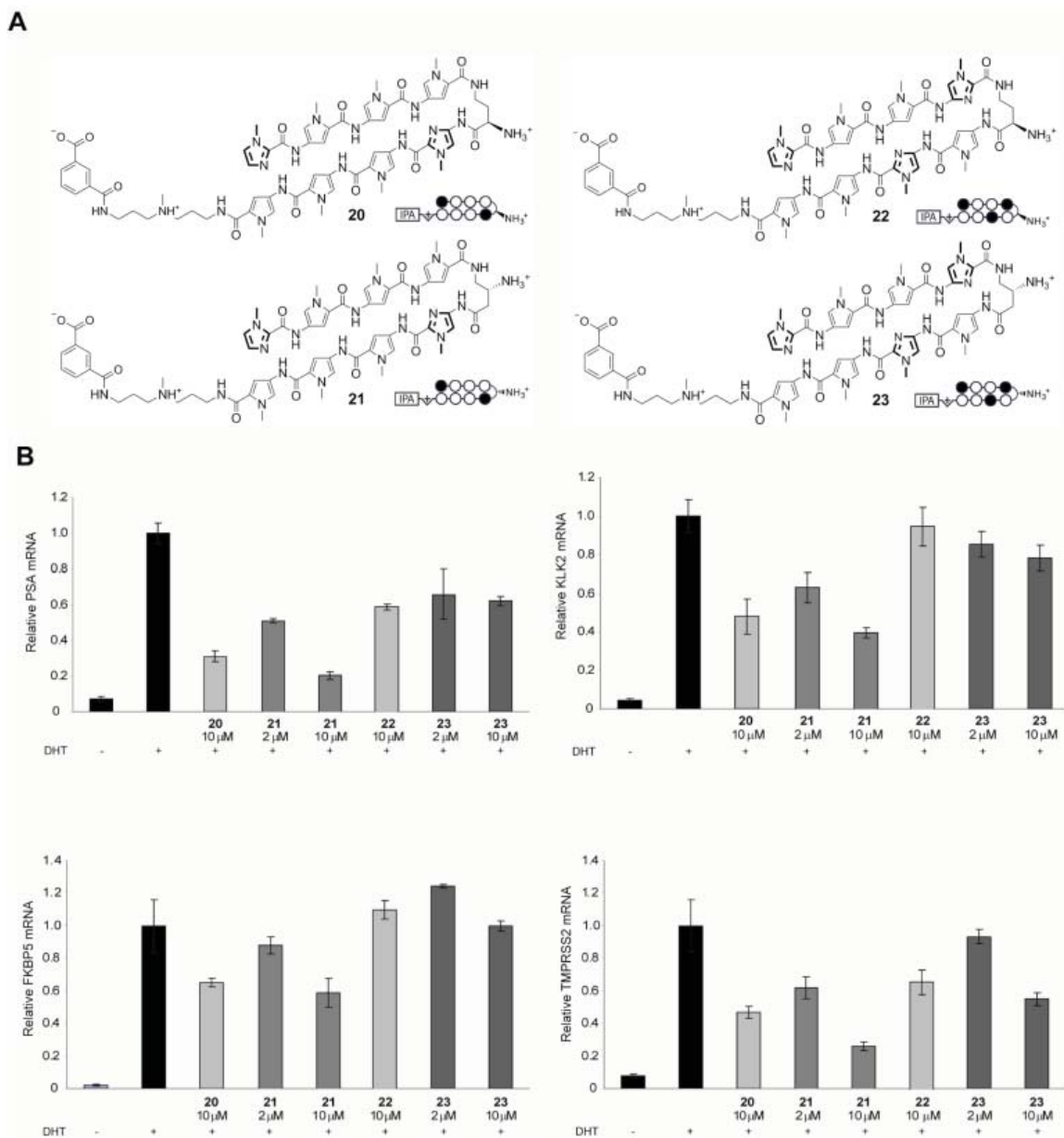


**Figure A.12** A) Chemical structures and ball-and-stick models of matched and mismatched polyamides **20-23**, respectively, targeted to 5'-AGAACA-3'. B) Inhibition of DHT-induced PSA, KLK2, FKBP5, and TMPRSS2 expression by **20-23** measured by quantitative real-time RT-PCR.